GeoHealth

RESEARCH ARTICLE

10.1029/2023GH000941

Key Points:

- The World Health Organization (WHO) updated cyanobacteria harmful algal blooms (cyanoHABs) guidelines for chlorophyll-*a* (chl-*a*) as a proxy
- With satellite remote sensing (SRS), we estimated and classified chl-*a* to compare cyanotoxins advisories used by California
- This study provides a framework for evaluating public health utility of SRS for enhancing cyanotoxin monitoring globally

Supporting Information:

Supporting Information may be found in the online version of this article.

Correspondence to:

B. N. Lopez Barreto,
blopezbarreto@ucmerced.edu

Citation:

Lopez Barreto, B. N., Hestir, E. L., Lee, C. M., & Beutel, M. W. (2024). Satellite remote sensing: A tool to support harmful algal bloom monitoring and recreational health advisories in a California reservoir. *GeoHealth*, *8*, e2023GH000941. https://doi.org/10.1029/2023GH000941

Received 3 SEP 2023
Accepted 31 JAN 2024

Author Contributions:

Conceptualization: Brittany N. Lopez Barreto, Erin L. Hestir, Christine M. Lee
Data curation: Brittany N. Lopez Barreto, Marc W. Beutel
Formal analysis: Brittany N. Lopez Barreto
Investigation: Brittany N. Lopez Barreto
Methodology: Brittany N. Lopez Barreto, Erin L. Hestir, Marc W. Beutel
Supervision: Erin L. Hestir, Christine M. Lee
Visualization: Brittany N. Lopez Barreto

Satellite Remote Sensing: A Tool to Support Harmful Algal Bloom Monitoring and Recreational Health Advisories in a California Reservoir

Brittany N. Lopez Barreto[1,2], Erin L. Hestir[1,2], Christine M. Lee[3], and Marc W. Beutel[1]

[1]Environmental Systems Graduate Group, Department of Civil & Environmental Engineering, University of California Merced, Merced, CA, USA, [2]Center for Information Technology Research in the Interest of Society, The Banatao Institute, University of California Merced, Merced, CA, USA, [3]NASA Jet Propulsion Laboratory, California Institute of Technology, Pasadena, CA, USA

Abstract Cyanobacterial harmful algal blooms (cyanoHABs) can harm people, animals, and affect consumptive and recreational use of inland waters. Monitoring cyanoHABs is often limited. However, chlorophyll-*a* (chl-*a*) is a common water quality metric and has been shown to have a relationship with cyanobacteria. The World Health Organization (WHO) recently updated their previous 1999 cyanoHAB guidance values (GVs) to be more practical by basing the GVs on chl-*a* concentration rather than cyanobacterial counts. This creates an opportunity for widespread cyanoHAB monitoring based on chl-*a* proxies, with satellite remote sensing (SRS) being a potentially powerful tool. We used Sentinel-2 (S2) and Sentinel-3 (S3) to map chl-*a* and cyanobacteria, respectively, classified chl-*a* values according to WHO GVs, and then compared them to cyanotoxin advisories issued by the California Department of Water Resources (DWR) at San Luis Reservoir, key infrastructure in California's water system. We found reasonably high rates of total agreement between advisories by DWR and SRS, however rates of agreement varied for S2 based on algorithm. Total agreement was 83% for S3, and 52%–79% for S2. False positive and false negative rates for S3 were 12% and 23%, respectively. S2 had 12%–80% false positive rate and 0%–38% false negative rate, depending on algorithm. Using SRS-based chl-*a* GVs as an early indicator for possible exposure advisories and as a trigger for in situ sampling may be effective to improve public health warnings. Implementing SRS for cyanoHAB monitoring could fill temporal data gaps and provide greater spatial information not available from in situ measurements alone.

Plain Language Summary Lakes often have algal blooms that create a water quality concern, especially when they contain cyanobacteria, which can be toxic to both humans and animals. These harmful algal blooms are of great concern in areas with limited water supply in states such as California. While it is often difficult and costly to collect and monitor toxin concentrations, monitoring concentrations of chlorophyll-*a* (chl-*a*) –a measure of how much algae are present—is relatively common and can even be accomplished using satellite remote sensing. There have been multiple studies that have found a relationship between toxins produced by cyanobacteria and chl-*a*. The World Health Organization (WHO) has recently released (2021) an updated release of their previous 1999 guidance values for toxin monitoring based on chl-*a* concentration. With satellite data, we were able to measure chl-*a* concentration in a major reservoir in California, and then classify the chl-*a* measurements into the WHO's guidance values for toxins. We compared the satellite-based guidance values to the public advisory levels currently set by the California Department of Water Resources. Our results indicate that SRS of chl-*a* is a reasonable substitute for cyanobacteria toxin advisories, and our framework can be applied to similar cyanobacteria dominated lakes.

1. Introduction

Harmful algal blooms (HABs) are defined as an increase in phytoplankton concentration that has an adverse impact on aquatic environments and/or people. When cyanobacteria, also known as blue-green algae, produce HABs, human and wildlife health are threatened because cyanobacteria often produce toxins (Smayda, 1997; Stumpf & Tomlinson, 2007). Freshwater HABs occur worldwide and acute exposure to the cyanotoxins created by cyanobacteria HAB events (cyanoHABs) can lead to gastrointestinal illness. Chronic exposure to cyanotoxins can lead to liver damage, and recreational exposure can result in respiratory and skin irritation (Erdner et al., 2008). Wildlife are also affected by exposure to toxins released during blooms that can lead to illness or

Writing – original draft: Brittany N. Lopez Barreto, Erin L. Hestir
Writing – review & editing: Erin L. Hestir, Christine M. Lee, Marc W. Beutel

death (Backer et al., 2013). Subsequent hypoxia in the water body following HABs may contribute to fish kills and other detrimental ecosystem effects (Paerl et al., 2011). A major goal of water management and public health authorities is to monitor and eventually forecast cyanoHABs at local, regional, national, and global scales to inform and protect public health (Schaeffer et al., 2018; Stroming et al., 2020).

Because of the human health concerns posed by cyanotoxins, the World Health Organization (WHO) has issued guidance on exposure to cyanoHABs. Until recently, a commonly used method was based on cell counts. Using a microscope, an analyst can directly assess the presence of cyanobacteria by counting the number of cells (Sklenar et al., 2016). While it is a relatively straightforward procedure, accurate quantification is time consuming and requires careful quality control (Chorus & Bartram, 1999). Because of the laborious and costly nature of this approach, other methods have been suggested by the WHO, such as using chlorophyll-*a* (chl-*a*) as a proxy for water bodies where blooms are dominated by cyanobacteria.

In the United States, various state and regional authorities also have guidance for public health exposure and warnings for drinking water reservoirs and recreational water bodies impacted by HABs. For example, in California (CA), the Department of Water Resources (DWR) is the responsible authority for monitoring HABs at key water intake structures, and issues guidance based on the concentration of four specific cyanotoxins: microcystins, saxitoxins, cylindrospermopsin, and anatoxin-a. The toxin concentrations are measured in the laboratory using analytical biochemistry assays (typically via enzyme-linked immunosorbent assay, ELISA, (Sklenar et al., 2016)). The voluntary guidance relies on the science presented in the California Office of Environmental Health Hazard Assessment's (OEHHA) risk assessment for microcystin, anatoxin-a and cylindrospermopsin (OEHHA, 2012). The trigger level of 0.8 μg/L microcystin prompts increased monitoring and the placement of a caution sign that advises people, pets and livestock be kept away from the water and scum. A trigger warning of 6 μg/L microcystins prompts a warning stating that swimming is not recommended, and that pets and livestock should be kept away from the water. Both of OEHHA's action levels are based on the short-term rat ecotoxicology study by Heinze (1999). The WHO (1999) suggests a concentration of 20 μg/L microcystin as a warning level for the protection of human health based on the sub-chronic mouse study by Fawell et al. (1994, 1999).

In recognition of the challenges associated with toxin monitoring, including access to specialized equipment, many studies have either used or promoted the use of other water quality variables that are much easier to measure (e.g., chlorophyll-*a*) as a proxy for potential toxin exposure (Chorus & Bartram, 1999; Hunter et al., 2009; Stumpf et al., 2016; Tebbs et al., 2013). The WHO has recently changed its guidance on public health warnings for exposure to toxins from cyanoHABs (Chorus & Welker, 2021), specifically linking chl-*a* to cyanotoxins in water bodies known to have cyanobacteria (Table 1). This has simplified monitoring for potential public exposure because chl-*a* is a readily measured water quality variable; it is easily monitored from a variety of accessible technologies, including laboratory-based spectrophotometry or fluorometry of water samples (Arvola, 1981; Basak et al., 2021; Johan et al., 2014), in situ optical fluorometry instruments (Campbell et al., 1998; Stirbet et al., 2018), and increasingly, satellite remote sensing (SRS) (Gons et al., 2002; Moses et al., 2012; O'Reilly & Werdell, 2019; Seegers et al., 2021; Stumpf & Tomlinson, 2007; Urquhart et al., 2017).

Of the measurement technologies available to measure chl-*a*, SRS offers unique capabilities: it provides continuous spatial coverage over large areas with systematic, repeated visits that can be collated into a time series. This can enable better understanding of spatial and temporal patterns of surface water quality. Chl-*a* has been successfully measured from satellites for decades (Gitelson, 1992; Wynne et al., 2008, 2010), and has been used to support detection of HABs (Anderson, 2009; Dekker et al., 2018; Kutser, 2009; Papenfus et al., 2020). Of the currently operational Earth observing satellites, the European Space Agency's (ESA) Sentinel-2 (S2) provides one of the best combinations of spatial, temporal, and spectral coverage for chl-*a* for inland waters (Bramich et al., 2021). S2 is a constellation of two satellites, Sentinel-2A and Sentinel-2B. Each has a 10-day repeating orbit and combined create a revisit time of 5-day over an area. Each S2 satellite carries a MultiSpectral Instrument (MSI) with 13 spectral bands that measure across the visible to shortwave infrared region. The spatial resolution of this satellite varies (10, 20, and 60-m) depending on the band. S2's "red-edge" bands (measuring within the visible red and near infrared) are well suited to chl-*a* detection by taking advantage of the spectral peak phytoplankton have near 700 nm. Spectral coverage in this range is beneficial for aquatic environments since colored dissolved organic matter (CDOM) and non-algal particles (NAP) can confound algorithms in shorter wavelength visible bands (Bramich et al., 2021; Gitelson, 1992; Gitelson et al., 2008).

Table 1
The Guideline Values (GVs) for Recreational Waters by the WHO and Advisories Set by the Department of Water Resources (DWR) for Cyanotoxins

Authority	Authority guideline level	Quantity	SRS guideline value classification
CA DWR[a] (basis of comparison for this study)	Caution	0.8–5.99 µg/L Microcystins	No alert
	Warning	6–19.99 µg/L Microcystins	Elevated alert
	Danger	20 µg/L ≤ Microcystins	Elevated alert
WHO21	GV for Microcystins for recreational waters	Chl-*a* ≤ 24 µg/L	No alert
		Chl-*a* ≥ 24 µg/L	Elevated alert
WHO99	Relatively low probability of adverse health effects	≤20,000 cyanobacterial cells/ml *or* ≤10 chl-*a* µg/L	No alert
	Moderate probability of adverse health effects	20,000–100,000 cyanobacterial cells/ml *or* 10.1–50 chl-*a* µg/L	Elevated alert
	High probability of adverse health effects	≥100,000 cyanobacterial cells/ml *or* ≥50 chl-*a* µg/L	Elevated alert

Note. Our classification for each guideline value for both agencies is defined in the table. [a]Recreational health advisory levels. Note: US EPA finished drinking water 10-day health advisory for adults is 1.6 µg/L Microcystins, CA drinking water acute notification level is 3 µg/L Microcystins.

Cyanobacteria contains a specific pigment, phycocyanin, which has an absorption maximum near 620-nm that allows for successful cyanobacteria estimation from some satellite sensors (Lunetta et al., 2015; Ruiz-Verdú et al., 2008; Wynne et al., 2008). Unfortunately, few current and operational satellites have the spectral resolution required to detect the phycocyanin absorption feature. Envisat's MERIS (Medium Resolution Imaging Spectrometer) was designed for aquatic targets and was used for cyanobacteria estimation from 2002 to 2012, when it was decommissioned. Sentinel-3's (S3) Ocean and Land Color Instrument was launched in 2016 and has the spectral bands to detect phycocyanin and enable estimates of cyanobacteria. S3 currently underpins an operational cyanoHABs monitoring system developed through a multi-agency effort led by the Environmental Protection Agency (EPA), called the Cyanobacteria Assessment Network (CyAN). Both MERIS and Sentinel-3 have suitable spectral resolution and frequent revisit time (1–2 days) that make them attractive for cyanoHAB monitoring, but their spatial resolution is limited (300 × 300-m pixels).

The use of chl-*a* and cyanobacteria pigments as reasonable proxies for toxin monitoring has been demonstrated by several studies across a range of different water bodies. Matthews (2014) used chl-*a* products from the MERIS sensor to demonstrate the ability to identify cyanobacteria-dominated blooms in one marine setting and, later, this was extended to three eutrophic reservoirs in South Africa (Matthews & Bernard, 2015). In Tomlinson et al. (2016), they used the Cyanobacteria Index (CI) to track HABs across lakes in Florida using and Seegers et al. (2021) expanded this effort across the United States. The relationship of chl-*a* and cyanobacteria has also been shown using spectrophotometry (Randolph et al., 2008; Sendersky et al., 2017).

The use of proxies is not without its limitations, however. The relationship between pigments such as chl-*a* and toxins can vary over time based on the dynamics of bloom formation and as species composition and dominance varies (Kudela et al., 2015). For example, Stumpf et al. (2016) showed that SRS of chl-*a* and phycocyanin can be used to estimate cyanobacterial toxins if a model is established between measured pigments and toxins. They found that a relationship can remain constant for days to weeks in a lake, but over longer periods the relationship can weaken and may lead to large errors. Furthermore, just because cyanobacteria are present does not mean that they are necessarily toxin producing (Carmichael, 2001) and cyanotoxins do not have any optically detectable characteristics, which limits monitoring. The United States 2007 National Lakes Assessment reported that detected or high chl-*a* rates does not always lead to cyanoHABs; they found that only 27% of cases that indicated a recreational WHO risk through cyanobacterial abundance, microcystin or chl-*a* had any actual cyanotoxin risk (Loftin et al., 2016).

Given the variability in SRS of chl-*a* and cyanobacteria as a proxy for assessing cyanotoxin risk, there remains a need to better quantify the uncertainty of proxies relative to public health advisory levels. The objective of this study is to evaluate SRS-based chl-*a* and cyanobacteria proxies for cyanotoxin health advisories using a major multi-use reservoir in California's water system, San Luis Reservoir (SLR), as a case study. This study utilizes

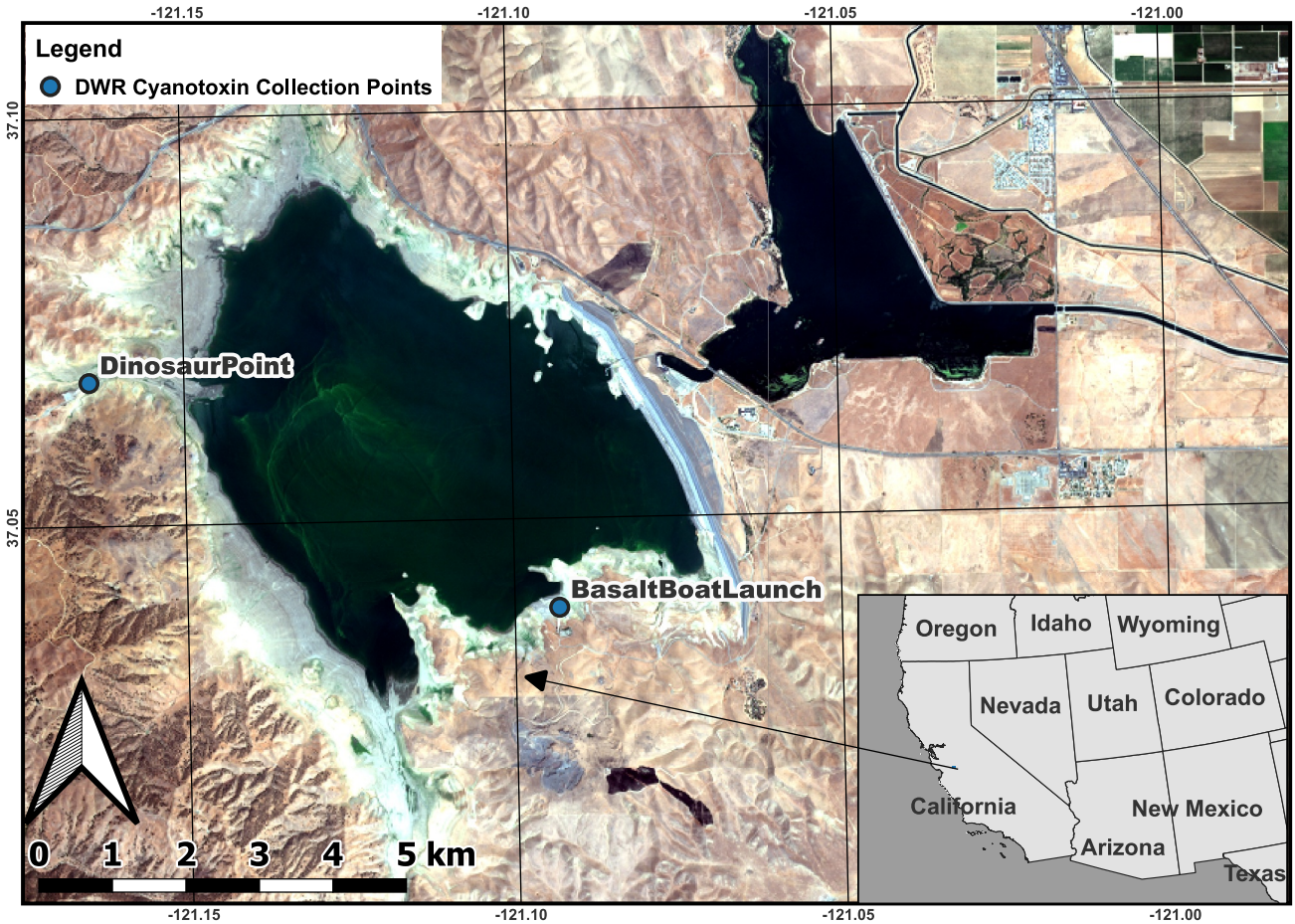

Figure 1. San Luis Reservoir in Los Banos, California, United States. Blue points are approximate locations where the California Department of Water Resources (DWR) measure cyanotoxins.

data from ongoing toxin monitoring conducted by the DWR to quantify the agreement between DWR toxin-based public health advisories and the new 2021 WHO (WHO21) chl-*a* based guideline values when applied to both field samples and SRS of chl-*a* from the S2 satellite sensors. We further evaluate the agreement between DWR advisories and the previous 1999 WHO (WHO99) cyanobacteria cell-count based guidance applied to the CyAN satellite product derived from the S3 satellite sensors.

2. Materials and Methods

2.1. Study Site

SLR is in the western San Joaquin Valley in CA and was created by the Bureau of Reclamation (Figure 1). It is the fifth largest reservoir in CA, the largest off-stream reservoir in the United States and is a key part of the State Water Project (SWP) and federal Central Valley Project (CVP) (United States Bureau of Reclamation, 2023). SLR is approximately 14-km from north to south and 8-km from west to east when full. The water level has an elevation height range of 105–165-m and the reservoir can hold approximately 2.5 km^3 of water (United States Bureau of Reclamation, 2023). The SWP is a water storage and delivery system that delivers water to about 27 million Californians and 750,000 acres of farmland and business throughout the state (California DWR, 2022), while the CVP serves another 2.5 million people and delivers water to approximately 3 million acres of the state's farms (United States Bureau of Reclamation, 2023). Water from SLR also serves the Santa Clara Valley Water District in the Southern San Francisco Bay Area, serving 15 cities with over 2 million residents (Santa Clara Valley Water, 2023). Most SLR water inflow is from man-made aqueducts which are supplied by northern California rivers. This reservoir grants flexibility for both water projects since it allows for state and federal water

storage when there is excess winter or spring flows from the Sacramento-San Joaquin Delta. SLR is also a popular destination for recreational fishing, boating, and swimming for locals.

Summers at SLR can see temperatures as high as 110°F (43°C) and winters as low as 32°F (0°C). The warm, low-pressure atmospheric conditions in the Central Valley brings cool ocean air from the Pacific Ocean that then produces strong wind and gust conditions that level off in the late afternoon. High winds tend to break apart thick mats of algae, limiting surface bloom formation. However, the high onshore winds at SLR mixes the water column leading to low stratification (Kraus et al., 2011), mobilizing deeper nutrients. These strong winds can lead to high temporal and spatial variability of blooms across the reservoir (Binding et al., 2018). Boat use closures are frequent due to high winds, which heavily impact monitoring within the reservoir. Algal blooms have been an increasing concern for SLR managers; the DWR has made multiple public announcements regarding dangerous toxin levels in recent years (CA DWR, 2022). SLR is a good candidate to evaluate chl-*a* as a proxy for cyanotoxin estimation based on the new WHO21 guideline values because of the well documented presence of cyanotoxins.

2.2. Toxin Monitoring Data

The DWR has conducted cyanotoxin monitoring at SLR since 2013. The DWR collects one surface water grab sample off the dock in SLR from Basalt Boat Launch or Dinosaur Point (dependent on road closures), and from a raw water tap from the upper intake of the Pacheco Pumping Plant (Figure 1). For this study, we used the surface water grab samples collected at Basalt Boat Launch to compare with our field data and SRS. While the DWR has collected cyanotoxins since 2013, the sampling was sparse (5–8 samples per year from 2013 to 2015). For our analysis, we used data from 2016 to 2022 due to the larger DWR data set during these years and coincident with the launch of Sentinel-2 in mid-2015.

The DWR begins to officially sample when there is a bloom sighting by the local rangers or if there is a notification made by the public. Not all initial visits have any toxin levels that trigger an advisory warning when the sampling period begins. On average, across the period of study, advisories were triggered on the first to third visit —beginning around May and lasting through October of each year. Monitoring can extend past October and is usually conducted until cyanotoxin levels falls below caution levels for two consecutive testing dates. Microcystin has been the only cyanotoxin detected during the period of record, except for a detection of anatoxin-a and cylindrospermopsin in August of 2022.

The DWR prepares their water samples by ultrasonication, where samples are inverted for 60 s to mix, then a subset is removed for algal identification purposes. The remaining samples are then sonicated to release toxins and prepared for analyses. In 2019, samples were freeze-thawed instead of sonicated. Sonication recommenced in 2020 (CA DWR, 2023). Toxin detection is performed using Enzyme-Linked Immunosorbent Assay (ELISA) techniques (United States Environmental Protection Agency, 2023). The DWR uses the microcystins/nodularins (ADDA) kit, which is designed to detect over 100 microcystin congeners identified to date (but cannot distinguish between congeners; United States Environmental Protection Agency, 2023). Data can be obtained for the cyanotoxins measurements in SLR through contacting the DWR's O & M Environmental Assessment Branch.

2.3. Chl-*a* Field Data Collection

We conducted four chl-*a* sampling events that occurred on the same day as a S2 satellite overpass and occurred within ±3 days of a DWR sampling event. Three of these trips were conducted during the 2021 bloom season when DWR performs regular monitoring (08/27/2021, 09/06/2021, and 09/23/2021). We added one field trip (05/01/2022) before the bloom season to characterize non-bloom conditions. The DWR began toxin monitoring 5 days earlier, on 04/25/2022 but found no toxins. The next DWR sampling event was not until 05/23/2022. Thus, for spring 2022 the match-up between DWR data and field and SRS S2 data was 5 days rather than three. A total of nine sampling events were attempted, but frequent reservoir closures due to high winds limited the number of match-up sampling events. Each sampling event started at approximately 9:30 a.m. PST and concluded about 11 a.m. PST to best match the time of mid-morning satellite overpasses (10:00 and 10:30 a.m. PST for S3 and S2, respectively). Surface water samples were collected from a utility boat and stored in 1-L Nalgene bottles. The bottles were kept in a cooler filled with ice and then refrigerated until laboratory analysis. Water collection sites were marked using a handheld Trimble Geo-XT GNSS unit. For the first sampling event, we collected triplicate samples at each site. Following analysis of the first round of samples, subsequent sampling events collected duplicate samples based on low sample variance.

For each sampling date, we visited pre-established sampling locations that were approximately 1-km apart. Due to wind conditions, we were unable to revisit the same location with high geolocational precision. The average distance of each sampling event from the pre-established sampling location was 56-m with a standard deviation of 36.6. An extra site was added for the 05/01/2022 sampling event because we wanted to include another sample closer to the edge of the reservoir while it was still full.

2.4. Laboratory Analysis of Chl-*a*

The refrigerated water samples were filtered following the EPA's Standard Operating Procedure for Chlorophyll-*a* Sampling and Analysis (EPA, 2023). All samples were processed within 24 hr of collection and shaken in case of settling. Volumes of water filtered ranged from 50 to 500 mL based on water quality conditions using Whatman glass microfiber filter pads. An absorption spectrophotometer (Visible Spectrophotometer 721 LDC Digital Lab Spectrophotometer) measuring at 665 and 750 nm with a 90% acetone extraction solution was used for chl-*a* measurement following standard methods (APHA, 2005).

2.5. Remotely Sensed Data

2.5.1. Chl-*a* Products From Sentinel-2

S2 level-1C (L1C) top of atmosphere (TOA) reflectance products from 01/01/2016 to 12/31/2022 that provided coverage for SLR (tile 10SFG) were downloaded from the ESA Copernicus online database. We filtered 10SFG images for less than 25% cloud cover and visually inspected each image to further ensure cloud-free conditions over the reservoir. This resulted in a S2 data set of 377 images.

Because of the absorption and scattering of light in the atmosphere, coupled with the overall low signal of water in SRS, atmospheric correction is crucial for water quality monitoring and assessment (Mobley et al., 2016; Seegers et al., 2021). The TOA data obtained from Copernicus were converted to aquatic remote sensing reflectance (Rrs) using ACOLITE version 20220222.0 software package (Vanhellemont & Ruddick, 2018). ACOLITE is an open-source software developed for aquatic applications. It applies the dark spectrum fitting method (DSF) for atmospheric correction, which determines the reflectance based on multiple dark targets in the image (Vanhellemont & Ruddick, 2018). This processor has been shown to be more effective for aquatic inland applications for S2 compared to other existing algorithms (Vanhellemont, 2019) and has been used in other inland aquatic studies (Bramich et al., 2021; Rodríguez-Benito et al., 2020; Theenathayalan et al., 2022), including in California (Lee et al., 2021). Images were resampled to 20-m and the default sunglint correction was applied.

We selected three commonly used chl-*a* algorithms shown to work well for inland waters: Mishra and Mishra (2012), Gons et al. (2002), and Moses et al. (2012). Mishra and Mishra (2012) use bands 4 and 5. Gons et al. (2002) uses bands 4 and 7 (with central wavelengths of approximately 665 and 780-nm, respectively) and the additional option ACOLITE provides by switching band 7 with band 6 (approximate central wavelength of 740-nm). Moses et al. (2012) is a 3-band model using bands 4, 5 (approximate central wavelength of 705-nm) and 7, with again the addition of switching band 7 with 6. For the Gons et al. (2002), Mishra and Mishra (2012), and Moses et al. (2012) algorithms, we used the published coefficients in our implementation.

Our criteria to consider a match-up for S2 images and DWR sampling is that both must be acquired on the same day. This resulted in a total of 38 S2 images that had a match-up with DWR for further comparison. While 38 out of 377 represents only 10% of available images, we limited the time frame for S2 and DWR data comparison for the same day because varying winds can lead to different bloom spatial variability, which could have influenced the results.

2.5.2. Cyanobacteria Cell Counts From Sentinel-3

Remote sensing-based cyanobacteria cell count products were obtained from the Cyanobacteria Assessment Network (CyAN), a collaborative project between the EPA, National Aeronautics and Space Administration (NASA), National Oceanic and Atmospheric Administration, and the United States Geological Survey. The CyAN products, CI_{cyano}, are based on the Cyanobacteria Index (CI) (Wynne et al., 2008), and modified by Lunetta et al. (2015). CyAN offers daily and 7-day maximum value composite CI_{cyano} products in GEOTIFF format. The daily product was used for this study. The CI data were produced from ESA's Envisat's MERIS (2002–2012) and Sentinel-3 OLCI (2016-present) satellite data. The NASA Ocean Biology Processing Group (2023) converted

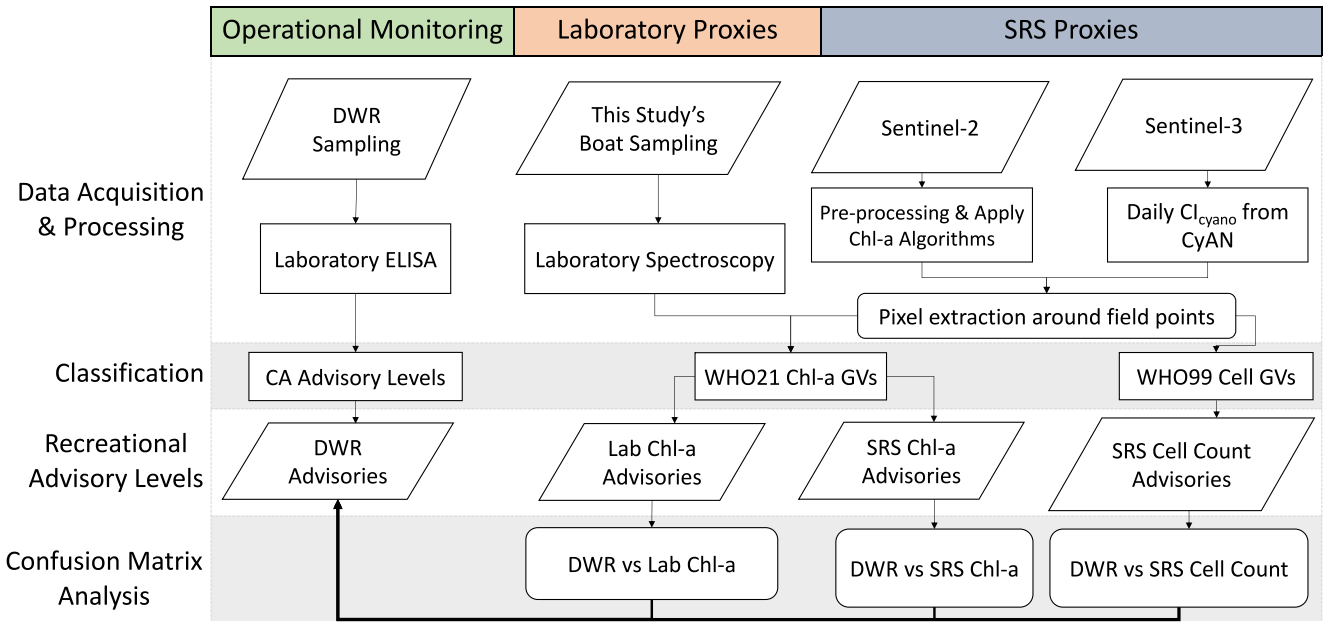

Figure 2. A representation of the approach used to examine agreement through confusion matrices between the California Department of Water Resources cyanotoxin advisories and laboratory/SRS chl-*a* and cyanobacteria classified by WHO GVs.

OLCI's Level-1B data to Level-3 Rayleigh-corrected reflectance, masking clouds and sunglint. Their output products have a land and mixed land-water mask. Data were downloaded from NASA's Ocean Color's CyAN File search for 2016–2022 on 01/15/2023 (https://oceandata.sci.gsfc.nasa.gov/api/cyan_file_search). We converted the downloaded data products from digital numbers to CI following Equation 1 (Lunetta et al., 2015; Wynne et al., 2008) and finally to cyanobacteria abundance following Equation 2 (Lunetta et al., 2015). Note that Equation 2 is the general estimate of cyanobacterial abundance, however CyAN's converted range is limited from ~10,000 to 7,000,000 cells/mL. From the S3 time series, we selected images over SLR that were acquired on the same day that a DWR sampling event occurred, resulting in 71 images.

$$\mathrm{CI}_{\mathrm{cyano}} = 10^{(3.0/(250.0 * \mathrm{Digital\ Number}) - 4.2)} \quad (1)$$

$$\mathrm{Cyanobacteria\ Abundance\ cells/mL} = \mathrm{CI}_{\mathrm{cyano}} * 1\mathrm{E} + 08 \quad (2)$$

2.5.3. Data Extraction and Time Series Development

We extracted the pixel values corresponding to our field sampling locations from the S2 chl-*a* and S3 cell count maps using the R raster package (R package version 3.5–15, Hijmans, 2022). For S2, the mean value in a 6 × 6 window (120-m) centered on the geolocation of each field sampling locations was extracted for each of the match-up dates in the time series. This spatial buffer was selected following a semi-variogram-based sensitivity analysis and follows findings from Sharp et al. (2021) who showed that critical scales of cyanobacterial blooms range from 70 to 175-m in a similar system (Clear Lake, CA). We did not incorporate any spatial buffer to the extraction of pixel values from the S3 maps since the pixel size is 300-m. These extractions were then used to create a time series of SRS-based chl-*a* and cyanobacteria abundance that could be compared against the DWR cyanotoxin monitoring data. Given the variability in geolocation for sampling stations between each field date, a different set of extractions was performed for each image date, with the window centered on the geolocation of the sampling station for that respective field date.

2.6. Data Analysis

To determine the agreement between the advisories suggested by the WHO and the DWR recreational health advisory levels, we created confusion matrices where a conceptual representation of the methods is shown in Figure 2.

2.6.1. DWR Versus S2 Chl-*a* or Lab Chl-*a*

First, we classified the chl-*a* data from both the field campaign and S2 into two categories: no alert (Chl-*a* ≤ 24 µg/L) or elevated alert (Chl-*a* ≥ 24 µg/L) based on the WHO21 Alert Level 2 GVs for recreational waters (Table 1). We then classified the DWR advisories at the "warning" or "danger" level as "elevated alerts." When DWR issued "caution" advisories, or when no advisory was issued, we classified these as "no alert." There were no "caution" DWR advisories during our field campaign dates, however there were cautions present for both S2 and S3 dates. The DWR and WHO21 classes were then compared in a confusion matrix that tabulates how many observations agree and disagree per class.

2.6.2. DWR Versus S3 Cyanobacteria Counts

The S3 cyanobacteria counts were classified using the WHO99 GVs (Table 1). WHO99 GVs of moderate or high probability of adverse health effects were classified as "elevated alert," and WHO99 GVs of relatively low probability were classified as "no alert." The classified data were then also compared with DWR advisories in a confusion matrix.

2.6.3. Confusion Matrix Analysis

To quantify the level of agreement between lab/SRS advisories and DWR advisories, we calculated the total agreement (TA), false positive rate (FPR), and false negative rate (FNR) from the confusion matrices. TA is the proportion of observations that agree on the level of advisory from both methods (i.e., SRS triggers an alert when the DWR indicates an elevated advisory) (Equation 3). If both advisory approaches agreed for every match-up, the TA value would be 100%. A disagreement would result in either a false positive or a false negative. The False Positive Rate (FPR) (Equation 3) is the probability that a false alarm would be raised, which for this study means that an alert by either lab or SRS would be triggered when there is no alert by the DWR. The False Negative Rate (FNR), often known as the miss rate, is the probability that either lab or SRS would not trigger an alert while the DWR would issue one.

$$\text{Total Agreement (TA)} = \frac{\text{True Positive} + \text{True Negative}}{\text{True Positive} + \text{False Positive} + \text{True Negative} + \text{True Negative}} \tag{3}$$

$$\text{False Positive Rate} = \frac{\text{False Positive}}{\text{False Positive} + \text{True Negative}} \tag{4}$$

$$\text{False Negative Rate} = \frac{\text{False Negative}}{\text{False Negative} + \text{True Positive}} \tag{5}$$

3. Results

3.1. DWR Cyanotoxin Monitoring

During the period of study, 41% of the DWR cyanotoxin monitoring visits resulted in "no advisory," and 59% of the sampling visits resulted in some form of advisory (Figure 3). The average duration of any triggered advisory (i.e., caution, warning, or danger) was 15.5 weeks for at least one site (Pacheco Pumping Plant and/or Dinosaur Point/Basalt Boat Launch). Warning or danger advisories for at least one site lasted an average duration of about 8 weeks, with high interannual variability. For example, in 2016 there were no consecutive warning or danger alerts, just two warning alerts for the year. However, sampling in 2016 was also minimal, with just seven visits for that year. The year with the greatest proportion of "danger" alerts was 2017, with about 20%, or 9 total alerts. The number of monitoring visits increased from 2016 to 2018; there were seven sampling visits for 2016, 29 in 2017, 19 in 2018, 32 in 2019, 26 in 2020, 29 in 2021, and 31 in 2022 (Figure 3).

3.2. Advisory Comparisons

Table 2 summarizes the total agreement, false positive and false negative statistics. S3 had the highest TA (83%), followed by S2 (79%), and then the lab-based chl-*a* samples (74%). FPR and FNR were highly variable between the lab-based and SRS-based approaches (Table 2).

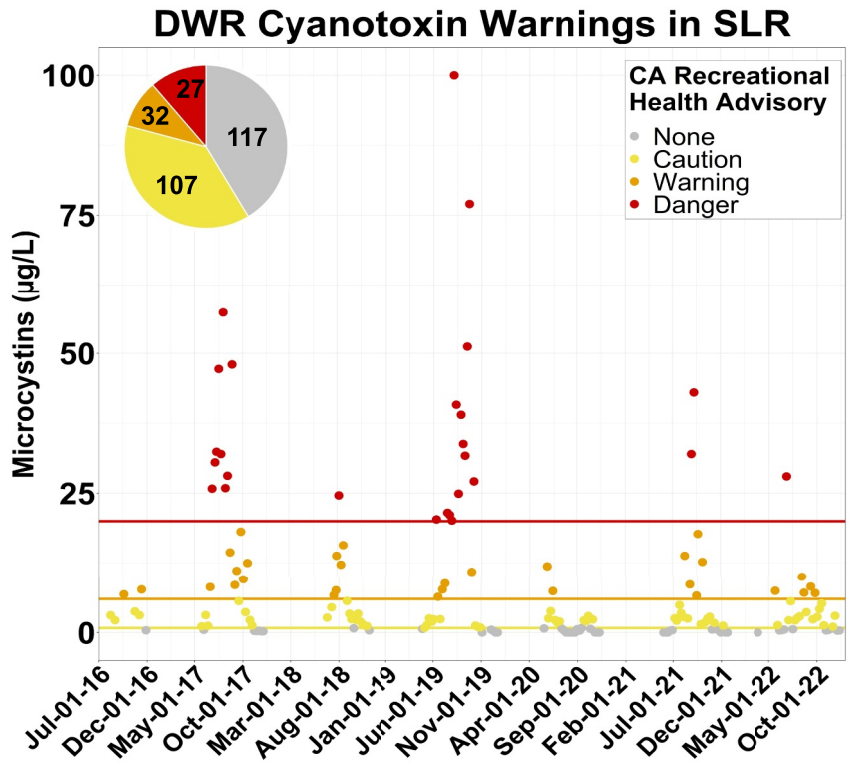

Figure 3. Microcystin samples collected from the CA DWR and determined via ELISA kits for 2016–2022 with indicated advisory levels.

Lab chl-*a*-based advisories had a TA of 74% with DWR advisories (or non-advisories) (Table 2). Of all the methods, the lab-based advisories had the lowest FPR; in only 10% of the match-ups, lab-based chl-*a* measurements would have triggered an advisory while DWR monitoring did not. However, the lab samples had high FNR; in 32% of the match-up cases, DWR monitoring triggered an advisory where advisories from lab chl-*a* samples would not. The chl-*a* range measured from the field campaigns was 1.6–311 µg/L, with an average of 54.8 µg/L and standard deviation of 76.2 µg/L. The chl-*a* values, summary statistics, and coordinates of the centroids for each sampling site can be found in Supporting Information S1. The date with the highest chl-*a* value was 09/06/2021 and the lowest value was from 05/01/2022. There was high spatial variability in chl-*a* measurements across the reservoir and across sampling dates (Figure 5). Across the four dates of field-collected samples for laboratory chl-*a*, about half would have triggered an advisory based on WHO21 (51%). From the three field dates in 2021 when SLR had higher bloom conditions, 68% of lab samples would have triggered a WHO21 advisory.

The TA between DWR and S2 advisories ranged from 51% to 79%, depending on algorithm used. The S2 chl-*a* algorithm that resulted in the highest TA was Mishra, followed by Gons and then Moses (Table 2). Moses had the

Table 2
The Total Agreement, False Positive and Negative Rate of WHO GV Classifications of Laboratory Chl-a, and SRS (Chl-a and Cyanobacteria) Compared to DWR Cyanotoxin Advisories at San Luis Reservoir, CA

Data source	Product	False positive (%)	False negative (%)	Total agreement (%)
Field Campaign	Laboratory	10	32	74.3
Sentinel-2 (20-m)	Mishra	12	38.4	78.9
	Moses	80	0	51.5
	Gons	45.8	15.4	67.6
Sentinel-3 (300-m)	CyAN	12.2	23.3	83.1

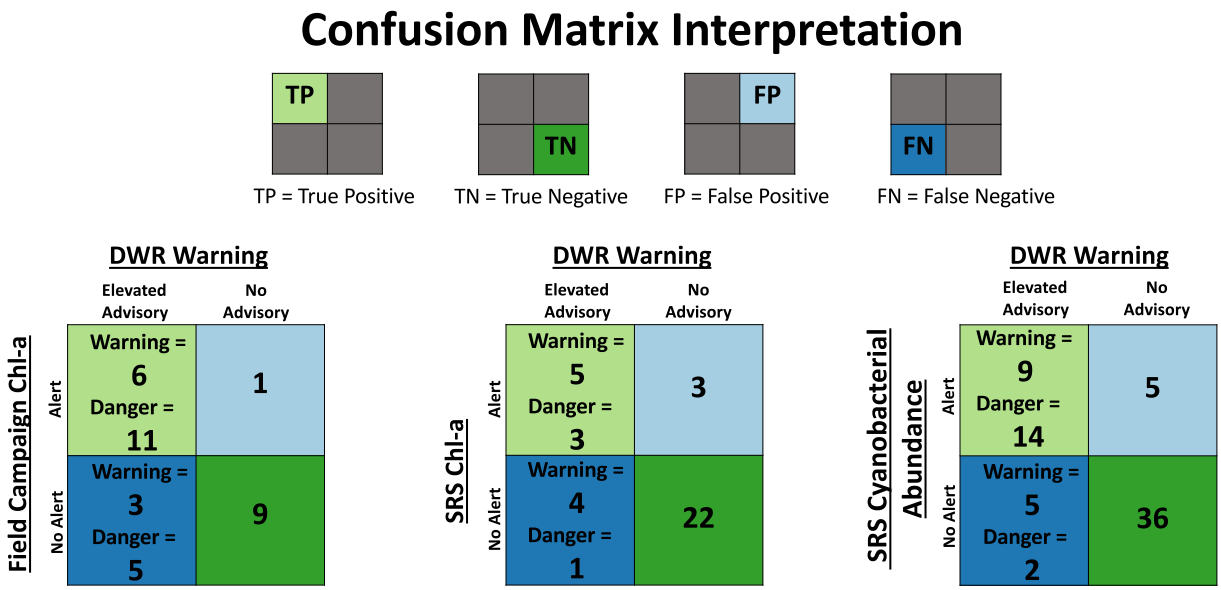

Figure 4. Confusion matrices comparing the field campaign samples, SRS Mishra, and CyAN to the advisory level determined by the DWR. SRS Mishra and CyAN are compared to the Basalt Boat Launch/Dinosaur Point location. The 05/01/2022 is not included since there was no DWR collection near that date.

highest FPR at 80% but had no false negative advisories. Gons and Moses's FPR were high (46% and 80% respectively). FNR for Gons and Mishra (15% and 38%, respectively) were similar or lower than lab chl-*a*-based advisories.

Of all proxies investigated, S3 had the highest overall TA: 83%. S3 FPR was similar to FPR values for lab and S2 Mishra. S3 had lower FNR than the lab samples, but S3 FNR was still higher than S2 Gons and S2 Moses. Of the 71 match-ups between S3 and DWR sampling events, there were 30 warning and danger DWR advisories, and in seven of these instances S3 resulted in no advisory. Figure 4 displays the confusion matrices of DWR alerts compared to alerts classified from lab-based chl-*a* samples, the best performing S2 algorithm, and S3.

There was high spatial variability within the reservoir across all proxy methods (Figure 5), indicating that a single advisory value does not apply to all areas. A spatial comparison of maps generated from S2, S3, and the field data shows that all proxy methods capture similar spatial patterns across the reservoir. Across the time series, northern portions of the reservoir tend to have fewer advisory conditions, whereas the middle-west portion (corresponding with sites 5 and 6) have the most frequent blooms. In general, areas of the reservoir where the lab chl-*a* indicated either an advisory or no advisory also match with SRS -based advisories, except for the September 23rd date. This exemplifies a case in which the S2 proxy indicates that the majority of the reservoir would be under advisory while the lab chl-*a* and S3 image showed regions where there would be no alert. The DWR did have an alert for SLR on this date. On 05/01/2022 there was no DWR alert, and all but one of the lab-based chl-*a* would not have triggered an advisory based on WHO21 GV. For 05/01/2022, S3 shows that most of the image had either no cyanobacteria present or levels too low to trigger any type of WHO99 alert. However, the S2 image indicates that large areas of the reservoir would not trigger an advisory apart from some small areas, especially in the southeastern part of the reservoir where S3 also had a few pixels indicating an alert.

3.3. SRS and DWR Time Series

Figure 6 visualizes the time series of cyanotoxins, chl-*a* and cyanobacterial cell abundance over the period of the study. The figure highlights the temporal correspondence of DWR-based cyanotoxin values with proxy values from S2 and S3 as well as the temporal density of SRS-based proxies, particularly Sentinel 3. The DWR sampling campaigns occur when cyanotoxins are expected to spike soon and finish when values fall below caution (Figure 6a). The greatest cyanotoxin values occur around July–September and the values tend to fall below caution around late October–December. While DWR monitoring is strategically conducted during peak algal

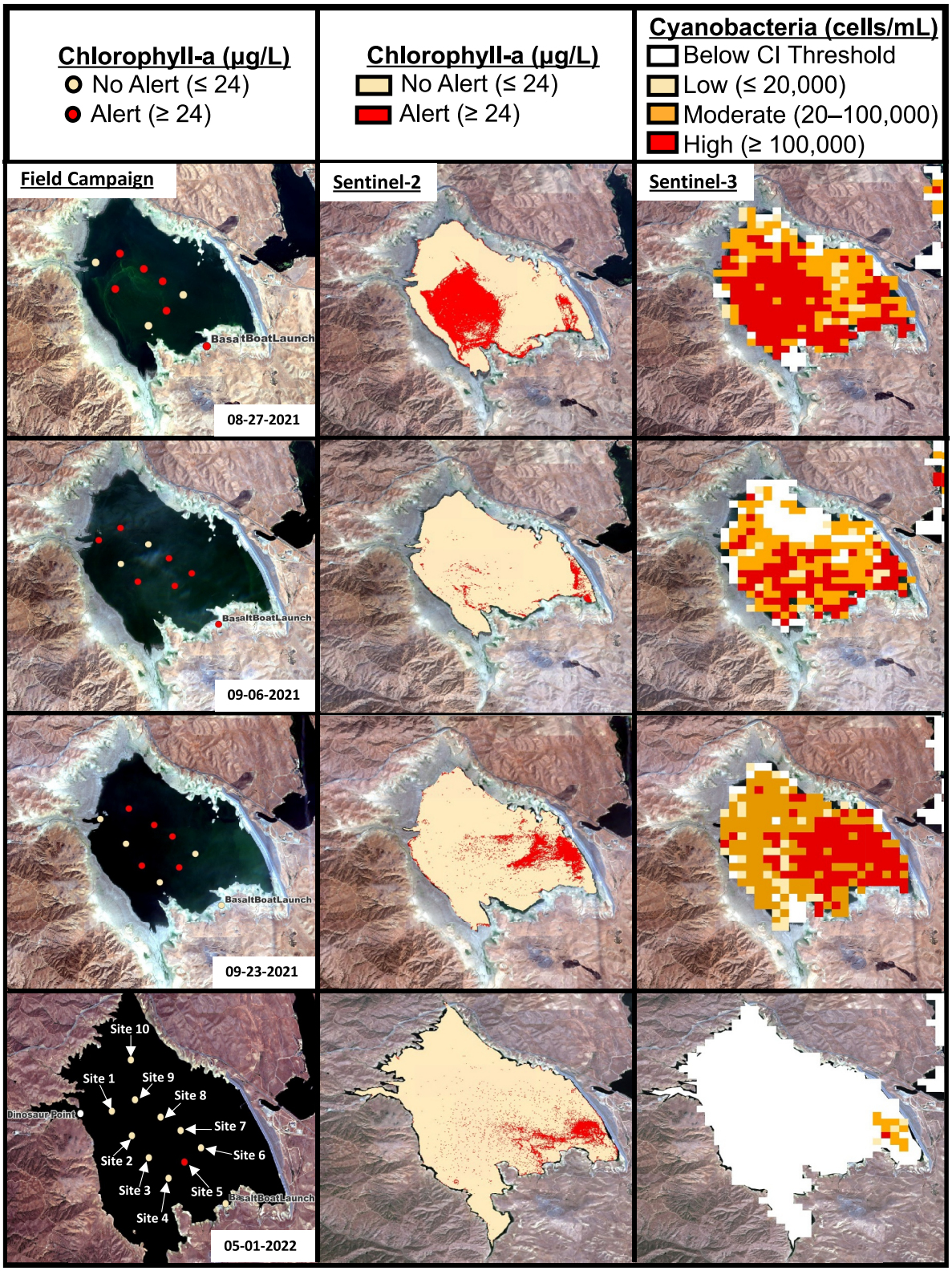

Figure 5. Left: field chl-*a* campaign points and DWR cyanotoxins color-coded based on WHO21 GVs (Table 1). Middle: S2 (Mishra)-based WHO21 GVs. Right: S3 (CyAN)-based WHO99 GVs where white pixels represent CI detection below threshold limits. For the purposes of this study the WHO99 GV of moderate and high were collapsed into a single class of alert.

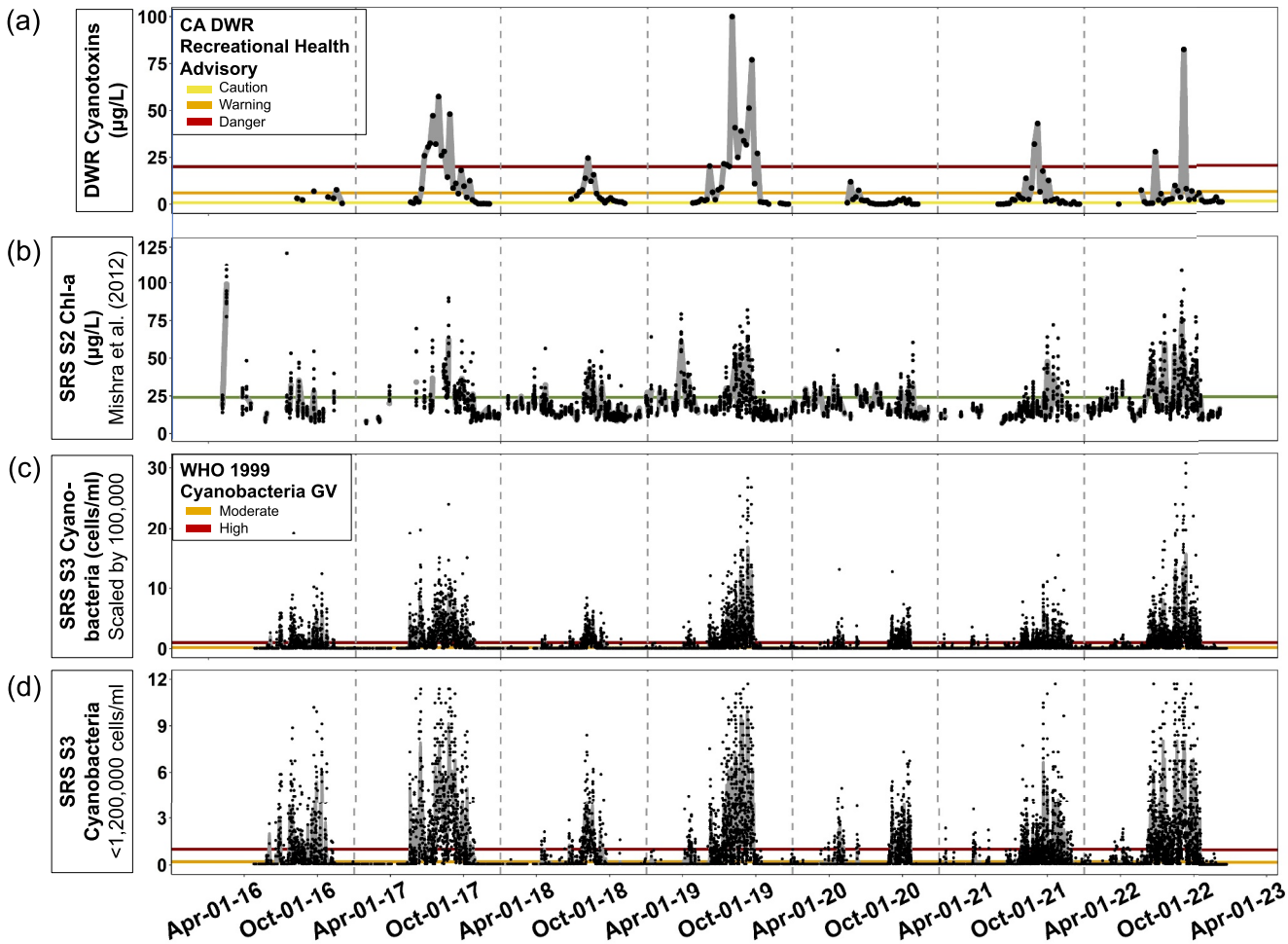

Figure 6. Dashed vertical lines indicate the beginning of a calendar year. (a) Cyanotoxins measured by the CA DWR with the state's recreational health advisory levels indicated by the horizontal lines. (b) Chl-*a* derived from Sentinel-2 using the Mishra and Mishra (2012) algorithm with the WHO21 recreational waters advisory value of 24 µg/L depicted as a green horizontal line. Chl-*a* *y*-axis limits are up to 125 µg/L, removing 5 outlier points. (c) Cyanobacteria abundance from Sentinel-3 with the WHO99 GVs on the horizontal scaled by 100,000. (d) Cyanobacteria abundance (from Sentinel-3) scaled on the *y*-axis for levels <1,000,000 cells/ml. Points for all graphs are the spatial mean of the day based on locations of field samples.

blooms seasons, it is evident that the absence of sampling during the remainder of the year may potentially miss conditions that would trigger an advisory.

The time series shows that the S2 chl-*a* (Mishra) results are mostly temporally concurrent with the DWR cyanotoxin time series (Figure 6b). The greatest chl-*a* values for S2 can be seen typically in July–August (Figure 6b), which is summer in California and typical for algal bloom trends. The lower S2 chl-*a* values where a WHO21 alert would be triggered generally ranges from October to April (Figure 6b). Much like the summarized in Table 2, there is agreement between the times when there were DWR danger levels and SRS chl-*a* values greater than 24 µg/L. Notably, there were times when SRS-based chl-*a* exceeded 24 µg/L, but there were no cyanotoxin data collected. While DWR cyanotoxin results tend to trigger some form of advisory in May, S2 chl-*a* exceeds 24 µg/L as early as February for all years. The S2 A/B satellites have a combined revisit time of 5 days, however, there are tiles that are excluded from the time series due to cloud, smoke or missing data within the images, which create data gaps in some parts of the year (Figure 6b). This is especially evident around December–April, which is winter and early spring in California when cloud cover and precipitation is higher.

S3 provides the most temporally dense time series since it has a daily revisit time. It is to be expected that S3 corresponds closely to DWR's findings since cyanotoxins ultimately originate from cyanobacteria. However, we

found that S3 had at least a moderate cyanobacteria abundance level starting in April, which is before the DWR typically samples.

4. Discussion

This study sought to evaluate the utility of SRS for cyanotoxin health advisories using SLR, a major multi-use reservoir in California, as a case study. This study found high rates of total agreement between public health advisories for cyanotoxin exposure in recreational waters issued by the CA DWR and proxy methods from both lab-based chl-*a* measurements and SRS. Over the period of study there were 71 match-ups between DWR cyanotoxin monitoring and S3, 38 match-ups with S2, and 4 match-ups with field sampling. With a total agreement of 83% for S3 and 79% for S2, SRS has good potential for augmenting cyanotoxin monitoring at SLR.

While the rate of false positives for S3 was low, S3 missed nearly one quarter (23%) of public health advisories that the DWR issued. However, these rates of false negatives may not solely be due to erroneous measurements by SRS, but rather spatial mismatch in sampling. With a 300-m spatial resolution, S3 may have difficulty resolving nearshore point sampling conducted by the DWR. The DWR's sampling is conducted off a dock (Basalt Boat Launch or Dinosaur Point; Figure 1), and there were multiple instances where a pixel was masked by CyAN because of its proximity to pixels classified as land (dock or shoreline). Thus, the closest available pixel may not represent the DWR sampling location or measurement. Furthermore, as visualized in Figure 5, there are many cases in which bloom conditions were present in some portions of the reservoir, but not necessarily at the locations of point-based sampling. The greatest advantage of using S3 for cyanotoxin warnings is its ability to directly approximate cyanobacteria abundance due to the position of its spectral channels as well as the near daily data it provides. Nonetheless, the 300-m pixel resolution limits the ability to resolve the spatial dynamics of cyanoHABS and precludes similar applications in smaller water bodies (Coffer et al., 2021; Schaeffer et al., 2022).

Encouragingly, S2 also had high rates of total agreement with DWR advisories; with a 20-m pixel resolution, the sensor is ideal for enhancing monitoring in smaller inland water bodies impacted by cyanoHABs. While S2 spatial capabilities are better than S3, the 5-day revisit time is less ideal for water quality measurements since they can vary day-to-day. However, when combined with DWR measurements, the sampling frequency for SLR would be about every 3 days. Despite this, cloud cover remains a persistent issue for both sensors. While S2 does not have the spectral capability of detecting cyanobacteria, other studies have also suggested the use of both, given what is known about the high correlation with chl-*a* concentration and cyanotoxins (Kislik et al., 2022; Rodríguez-Benito et al., 2020). Rodríguez-Benito et al. (2020) proposed the use of S3 as an operational surveillance mode at mesoscale and then, when there is a positive chl-*a* detection, they suggested implementing S2 to locate the areas of bloom. While their paper focused on chl-*a* only, the same idea could be used in the case for cyanotoxin monitoring to inform and augment DWR monitoring efforts, whereby S3 could be used to detect high concentrations of cyanobacteria cells on a near-daily basis and the higher spatial resolution of S2 could be used to help inform the timing and location of DWR sampling efforts, potentially issue earlier warnings while awaiting lab results, and targeting warnings to certain recreational areas most likely to be impacted by the bloom. While the spatially limited sampling locations for DWR is understandable due to financial, time and access constraints, it is still very likely that during times the DWR collects no or low levels of cyanotoxins from their sampling stations, there are other areas of SLR that may harbor conditions warranting an advisory. With the short time period between overpass and CyAN products available, S3 can be easily integrated in the DWR sampling plans. S2 has images available the day after overpass; however, there are no operational chl-*a* products suitable for inland waters available yet, and further development would be needed to operationally support a monitoring program.

The time series of different cyanoHAB proxy indicators (Figure 6) further indicates the utility of SRS in augmenting or complementing routine toxin monitoring. Overall, we observed that peaks in chl-*a* concentration and high cyanobacteria cell abundance levels measured by SRS coincide with periods when DWR has confirmed cyanotoxin presence. However, SRS provides data at a regular sampling interval that occurs year-round, whereas the current DWR program typically samples between May and October, during “bloom” season, which results in substantially fewer observations and alerts. In some years, such as early 2018 and 2020, SRS indicated that possible recreational advisories were occurring before DWR monitoring commenced for the season. Thus, while SRS also does not provide a complete time series due to cloud cover (which has a winter seasonal bias in this system), it can still be used to supplement cyanoHAB monitoring, particularly when

and where field sampling is not occurring. While some out-of-season alerts may be due to overprediction errors, some may also be due to real bloom occurrences that were not observed and reported to DWR to commence monitoring due to their location on the reservoir.

4.1. S2 Chl-*a* Algorithm Impacts

The choice of chl-*a* algorithm had a substantial impact on the total agreement as well as rates of false positives and false negatives. We would recommend the use of Mishra for San Luis Reservoir to augment cyanotoxin monitoring efforts based on the highest total agreement and lowest rate of false positive. However, further investigation in testing different algorithms, or the same algorithms used in our study, with more field data would strengthen these recommendations. Underestimation of chl-*a* is a well-documented challenge for SRS of inland waters that have high chl-*a* concentrations. The Mishra and Mishra (2012) algorithm was originally developed with in situ chl-*a* values ranging from 0.9 to 28.2 µg/L. Bramich et al. (2021) found that using the Normalized Difference Chlorophyll Index (NDCI), which is what the Mishra algorithm is built upon, underestimated chl-*a* measurements especially when samples were greater than 30 µg/L. Recently, Tóth et al. (2021) used ACOLITE and tested the Gons, Mishra, and Moses algorithms on S2 satellite data and found that SRS data overestimated chl-*a* if it was low (<10 µg/L) and underestimated chl-*a* if it was too high (values ranged up to 653 µg/L). Algorithms such as Mishra specifically use formulations that combine reflectance data measured in both the red and near-infrared portions to be more robust to confounding water quality factors such as CDOM and other non-algal particulate matter such as suspended sediments that contribute to the overall turbidity of the water. Despite this, others have also reported that these algorithms using this band to tend to overestimate chl-*a* for low values (∼5 µg/L) (Pahlevan et al., 2020; Werther et al., 2022).

Another possible explanation for when S2 chl-*a* algorithms under-predicted public health advisories may be due to the 2021 WHO GV's new threshold reasoning for chl-*a*. The second edition “Toxic Cyanobacteria in Water” states that the value for chl-*a* is much more conservative compared to the WHO99 GVs. They also state that in most field scenarios, cyanotoxin levels should be lower than given by the GV. They comment that local areas that understand their cyanobacterial population should set their own alerts. While California's DWR set their own advisory levels, they have used the previous WHO99 GVs as the reference for their warning and danger level. Whether it is more consequential to under or overpredict advisories should be weighed: the WHO21 GVs err on the side of lower chl-*a* threshold values to ensure that blooms are not underestimated.

The WHO21 framework supports parameters that are more locally or nationally accessible for cyanoHABs proxies. Along with chl-*a*, they have also recommended parameters such as Secchi disk depth or turbidity, two popularly measured water clarity indicators, as proxies for cyanoHABs (Chorus & Welker, 2021). Turbidity has been measured successfully through satellite remote sensing for decades (Choubey, 1992; Dogliotti et al., 2015; Moore, 1980; Nechad et al., 2009). While this study only focused on chl-*a* and CIs as proxies, future research could also investigate the utility of SRS-based turbidity for recreational alerts, and potentially a combined alert system that leverages both SRS-based chl-*a* and turbidity.

4.2. Consequences of False Negative and False Positive Public Health Advisories

While a high total agreement is the most ideal in the analysis, the performance of these proxies in terms of false negative and false positive advisories has consequences on information for the public to protect health and safety. A proxy method for cyanoHAB advisories that tends to overpredict blooms would maintain a conservative approach that prioritizes public safety. However, imposing multiple reservoir closures when there are no actual cyanoHAB events could lead to incurred costs for unnecessary water treatment or pumping interventions, fishing license and tourism revenue loss and general inconvenience to local and visiting recreational users (Wolf et al., 2017). CyanoHAB presence and cyanoHAB advisories can lead to millions of dollars in lost revenue annually for states that rely on tourism and recreation for revenue (Hoagland et al., 2002; Stroming et al., 2020). With high rates of false positive advisories, water managers may lose trust in monitoring technologies, and the community might lose trust in local and state authorities.

Unnecessary closures are not ideal and may incur costs, but those that become ill due to cyanoHAB exposure also incur a cost. There is limited literature and data on the financial cost of cyanoHAB-related illness, however DeFlorio-Barker et al. (2018) estimated the social cost of an individual to develop a gastrointestinal illness from a cyanoHAB to range from $10 to just over $300,000 in 2007 dollars. The lower value is based on typical over-the-

counter medicine while the much higher price is associated with severe hospitalization. A follow up study by Stroming et al. (2020) adjusted this cost to exclude potential loss of life since cyanoHABs cannot be directly linked with death. Their new adjusted cost was $11 for mild, $264 for moderate, and $10,700 per person for severe gastrointestinal illnesses linked to cyanoHABs. Further, frequent failure to issue public health advisories in the presence of a cyanoHAB may also erode manager and public trust. Thus, while false positive advisories may have economic and perceptual consequences, favoring proxies that minimize false negatives would help prevent potential cyanoHAB related illnesses. In this study, the S2 Mishra chl-*a* algorithm had higher rates of total agreement relative to the Gons algorithm (79% and 68%, respectively). However, Gons had lowers rates of false negatives, while Mishra had lower rates of false positives. Which algorithm is selected for enhanced monitoring, and whether that is ultimately used to issue public advisories is dependent on what is considered is more important to the user, minimizing the potential for illness, or minimizing unnecessary costs and impacts to recreation.

4.3. Strengths and Limitations of the Study

SRS for cyanoHAB alerts provides spatially explicit mapping capability and additional monitoring throughout the year, inclusive of typical bloom seasons. Some of the disagreement between the SRS and DWR alert levels may be due to the high spatial variability of the blooms. Because of the strong winds, the spatial variability of blooms in this reservoir are high, meaning DWR samples collected from one side of the reservoir may not be indicative of the entire reservoir. Ultimately, the DWR samples are taken at only a few point locations at the shore of the reservoir (Figure 1) (and one from a tap), whereas S3 has 100s of pixels in the reservoir, and S2 has >60,000 pixels measuring the reservoir. While the last day of our field campaign (05/01/2022) did have overall low values compared to the other dates, there was one sample that would have triggered an alert according to the WHO21 GV. As noted in our results, site five had high chl-*a* concentration, but there were no DWR toxin values for comparison. If there were DWR data for comparison, the sample would have been collected from a dock or at Pacheco Pumping Plant, which is on the opposite side of the reservoir from site five. From the S2 imagery shown in Figure 5, it is evident that these blooms form in different areas of the reservoir, where toxin sampling by the DWR would miss the event. This illustrates an important potential utility of remote sensing since it can measure areas where DWR does not, and during the times of the year they do not measure.

We have already seen great success with S3's CyAN products being used to reduce public exposure to cyanoHABs by guiding where to sample water quality and implement beach closures in states such as Utah, Wyoming, Oregon and New Jersey (NJDEP, 2020; OHA, 2023; Schaeffer et al., 2018; Seegers et al., 2021; WDEQ, 2022). The CyAN project has created an app that is the first of its kind to provide cyanoHAB data products to water quality managers for both recreational and drinking water sources in a cost-effective way (Schaeffer et al., 2018). In a recent study by Mishra et al. (2021) it was reported that data from CyAN had 84% bloom agreement detection across lakes from 11 states in the contiguous United States, a value remarkably similar to the findings from this study (83% overall agreement).

The current latency of water quality products is not always ideal for public health advisories, which are expected to represent the most up-to-date conditions. Field sampling and laboratory analysis of chl-*a* may be a reliable and simpler method than using SRS, however, it is also a slower process with smaller spatial coverage compared to using SRS. With field data, the time to collect samples and transport them back to a lab for analysis may take longer than using SRS data. ESA S2 images and NASA S3 CyAN products are available the next day of satellite overpass via their website (oceandata.sci.gsfc.nasa.gov/api). The availability of data is time sensitive for the issuance of public health advisories, so methods such as SRS that can provide quick and reliable measurements are necessary for enhancing monitoring.

5. Conclusion

The main takeaway from this research is that SRS can become an important tool for monitoring potential cyanotoxin exposures in cyanobacteria dominated lakes nationally or globally. This study assessed how well various proxies for public health advisories for cyanotoxin exposure agree with current government monitoring approaches. This study examined how well the recent WHO21 GVs work for using chl-*a* as a proxy for cyanotoxins and assessed the utility of SRS as a measurement modality for this proxy. The WHO21 GVs are relatively new and to the knowledge of the authors of this paper, have not been extensively explored in the context of SRS as of this study. Our results suggest that using SRS of chl-*a* is an acceptable proxy for predicting potential exposure to

cyanotoxins from cyanoHABs. Our findings support previous research showing high rates of agreement between S3 and cyanoHABs. Further, we found that using the WHO21 GV was nearly as successful as using S3-based SRS based on the prior WHO99 GVs focused on cyanobacteria cell counts. Integrating SRS data with concurrent in situ monitoring could create a cohesive time series for any lake such as San Luis Reservoir, an important instrument in California's water supply.

Conflict of Interest

The authors declare no conflicts of interest relevant to this study.

Data Availability Statement

Data created and used for this paper (except for the remote sensing images) are available at the Mendeley Data repository (Lopez Barreto, 2023), where it is free to access and use with no registration required. The files associated with this data set are licensed under a Creative Commons Attribution 4.0 International license. The list of names of all satellite remote sensing images used are found in our repository.

Acknowledgments
This study was supported by grants from NASA Future Investigators in NASA Earth and Space Science and Technology (FINESST) (No. 80NSSC21K622), NASA Jet Propulsion Laboratory Water Resources group, and University of California Merced's Center for Information Technology Research in the Interest of Society & the Banatao Institute (CITRIS). We would like to thank Julia Burmistrova, Dulcinea Avouris, Jacob Nesslage, and Nicholas Martinez for their help with field work and/or the processing of the chlorophyll-*a* samples. We would also like to thank the two anonymous reviewers for providing constructive comments and suggestions, which improved the quality of the manuscript.

References

American Public Health Association (APHA), American Water Works Association (AWWA), and Water Environment Federation (WEF). (2005). *Standard methods for the examination of water and wastewater* (21st ed.). APHA.

Anderson, D. M. (2009). Approaches to monitoring, control and management of harmful algal blooms (HABs). *Ocean & Coastal Management*, *52*(7), 342–347. https://doi.org/10.1016/j.ocecoaman.2009.04.006

Arvola, L. (1981). Spectrophotometric determination of chlorophyll a and phaeopigments in ethanol extractions. *Annales Botanici Fennici*, *18*(3), 221–227. Retrieved from http://www.jstor.org/stable/23725236

Backer, L. C., Landsberg, J. H., Miller, M., Keel, K., & Taylor, T. K. (2013). Canine cyanotoxin poisonings in the United States (1920s-2012): Review of suspected and confirmed cases from three data sources. *Toxins*, *5*(9), 1597–1628. https://doi.org/10.3390/toxins5091597

Basak, R., Wahid, K. A., & Dinh, A. (2021). Estimation of the chlorophyll-a concentration of algae species using electrical impedance spectroscopy. *Water*, *13*(9), 1223. https://doi.org/10.3390/w13091223

Binding, C. E., Greenberg, T. A., McCullough, G., Watson, S. B., & Page, E. (2018). An analysis of satellite-derived chlorophyll and algal bloom indices on Lake Winnipeg. *Journal of Great Lakes Research*, *44*(3), 436–446. https://doi.org/10.1016/j.jglr.2018.04.001

Bramich, J., Bolch, C. J. S., & Fischer, A. (2021). Improved red-edge chlorophyll-a detection for Sentinel 2. *Ecological Indicators*, *120*, 106876. https://doi.org/10.1016/j.ecolind.2020.106876

California Department of Water Resources (CA DWR) Operations & Maintenance Environmental 739 Assessment Branch. (2023). Cyanotoxin results—Methods.

California Department of Water Resources (CA DWR). (2022). State water project. Retrieved from https://water.ca.gov/Programs/State-Water-Project?yearMonth=201911&upcoming=false

Campbell, D., Hurry, V., Clarke, A. K., Gustafsson, P., & Oquist, G. (1998). Chlorophyll fluorescence analysis of cyanobacterial photosynthesis and acclimation. *Microbiology and Molecular Biology Reviews: Microbiology and Molecular Biology Reviews*, *62*(3), 667–683. https://doi.org/10.1128/MMBR.62.3.667-683.1998

Carmichael, W. W. (2001). Health effects of toxin-producing cyanobacteria: "The CyanoHABs". *Human and Ecological Risk Assessment: An International Journal*, *7*(5), 1393–1407. https://doi.org/10.1080/20018091095087

I. Chorus, & J. Bartram (Eds.) (1999). *Toxic cyanobacteria in water*. https://doi.org/10.1201/9781482295061

I. Chorus, & M. Welker (Eds.) (2021). *Toxic cyanobacteria in water* (2nd ed.). CRC Press.

Choubey, V. K. (1992). Correlation of turbidity with Indian remote sensing Satellite-1A data. *Hydrological Sciences Journal*, *37*(2), 129–140. https://doi.org/10.1080/02626669209492573

Coffer, M. M., Schaeffer, B. A., Foreman, K., Porteous, A., Loftin, K. A., Stumpf, R. P., et al. (2021). Assessing cyanobacterial frequency and abundance at surface waters near drinking water intakes across the United States. *Water Research*, *201*, 117377. https://doi.org/10.1016/j.watres.2021.117377

DeFlorio-Barker, S., Wing, C., Jones, R. M., & Dorevitch, S. (2018). Estimate of incidence and cost of recreational waterborne illness on United States surface waters. *Environmental Health*, *17*(1), 3. https://doi.org/10.1186/s12940-017-0347-9

Dekker, A. G., Pinnel, N., Gege, P., Briottet, X., Court, A., Peters, S., et al. (2018). Feasibility study for an aquatic ecosystem Earth observing system version 1.2. In *Feasibility study for an aquatic ecosystem Earth observing system*. Retrieved from https://hal.science/hal-02172188

Dogliotti, A. I., Ruddick, K. G., Nechad, B., Doxaran, D., & Knaeps, E. (2015). A single algorithm to retrieve turbidity from remotely-sensed data in all coastal and estuarine waters. *Remote Sensing of Environment*, *156*, 157–168. https://doi.org/10.1016/j.rse.2014.09.020

Environmental Protection Agency (EPA). (2023). Standard operating procedure for chlorophyll a sampling method field procedure, revision 07. Retrieved from https://www.epa.gov/sites/default/files/2017-01/documents/sop-for-chlorophyll-a-201303-5pp.pdf

Erdner, D., Dyble, J., Parsons, M., Stevens, R., Hubbard, K., Wrabel, M., et al. (2008). Centers for oceans and human health: A unified approach to the challenge of harmful algal blooms. *Environmental Health: A Global Access Science Source*, *7*(2), S2. https://doi.org/10.1186/1476-069X-7-S2-S2

Fawell, J., Cp, J., & James, H. (1994). Toxins from blue-green algae: Toxicological assessment of microcystin-LR and a method for its determination in water.

Fawell, J. K., Mitchell, R. E., Hill, R. E., & Everett, D. J. (1999). The toxicity of cyanobacterial toxins in the mouse: II anatoxin-a. *Human & Experimental Toxicology*, *18*(3), 168–173. https://doi.org/10.1177/096032719901800306

Gitelson, A. (1992). The peak near 700 nm on radiance spectra of algae and water: Relationships of its magnitude and position with chlorophyll concentration. *International Journal of Remote Sensing*, *13*(17), 3367–3373. https://doi.org/10.1080/01431169208904125

Gitelson, A. A., Dall'Olmo, G., Moses, W., Rundquist, D. C., Barrow, T., Fisher, T. R., et al. (2008). A simple semi-analytical model for remote estimation of chlorophyll-a in turbid waters: Validation. *Remote Sensing of Environment*, *112*(9), 3582–3593. https://doi.org/10.1016/j.rse.2008.04.015

Gons, H. J., Rijkeboer, M., & Ruddick, K. G. (2002). A chlorophyll-retrieval algorithm for satellite imagery (Medium Resolution Imaging Spectrometer) of inland and coastal waters. *Journal of Plankton Research*, *24*(9), 947–951. https://doi.org/10.1093/plankt/24.9.947

Heinze, R. (1999). Toxicity of the cyanobacterial toxin microcystin-LR to rats after 28 days intake with the drinking water. *Environmental Toxicology*, *14*(1), 57–60. https://doi.org/10.1002/(SICI)1522-7278(199902)14:1<57::AID-TOX9>3.0.CO;2-J

Hijmans, R. J. (2022). raster: Geographic data analysis and modeling. Retrieved from https://cran.r-project.org/package=raster

Hoagland, P., Anderson, D. M., Kaoru, Y., & White, A. W. (2002). The economic effects of harmful algal blooms in the United States: Estimates, assessment issues, and information needs. *Estuaries*, *25*(4), 819–837. https://doi.org/10.1007/BF02804908

Hunter, P. D., Tyler, A. N., Gilvear, D. J., & Willby, N. J. (2009). Using remote sensing to aid the assessment of human health risks from blooms of potentially toxic cyanobacteria. *Environmental Science & Technology*, *43*(7), 2627–2633. https://doi.org/10.1021/es802977u

Johan, F., Mat Jafri, M. Z., Lim, H. S., & Wan Omar, W. M. (2014). Laboratory measurement: Chlorophyll-a concentration measurement with acetone method using spectrophotometer. In *IEEE international conference on industrial engineering and engineering management, 2015* (pp. 744–748). https://doi.org/10.1109/IEEM.2014.7058737

Kislik, C., Dronova, I., Grantham, T. E., & Kelly, M. (2022). Mapping algal bloom dynamics in small reservoirs using Sentinel-2 imagery in Google Earth Engine. *Ecological Indicators*, *140*, 109041. https://doi.org/10.1016/j.ecolind.2022.109041

Kraus, T. E. C., Bergamaschi, B. A., Hernes, P. J., Doctor, D., Kendall, C., Downing, B. D., & Losee, R. F. (2011). How reservoirs alter drinking water quality: Organic matter sources, sinks, and transformations. *Lake and Reservoir Management*, *27*(3), 205–219. https://doi.org/10.1080/07438141.2011.597283

Kudela, R. M., Palacios, S. L., Austerberry, D. C., Accorsi, E. K., Guild, L. S., & Torres-Perez, J. (2015). Application of hyperspectral remote sensing to cyanobacterial blooms in inland waters. *Remote Sensing of Environment*, *167*, 196–205. https://doi.org/10.1016/j.rse.2015.01.025

Kutser, T. (2009). Passive optical remote sensing of cyanobacteria and other intense phytoplankton blooms in coastal and inland waters. *International Journal of Remote Sensing*, *30*(17), 4401–4425. https://doi.org/10.1080/01431160802562305

Lee, C. M., Hestir, E. L., Tufillaro, N., Palmieri, B., Acuña, S., Osti, A., et al. (2021). Monitoring turbidity in San Francisco Estuary and Sacramento–San Joaquin delta using satellite remote sensing. *JAWRA Journal of the American Water Resources Association*, *57*(5), 737–751. https://doi.org/10.1111/1752-1688.12917

Loftin, K. A., Graham, J. L., Hilborn, E. D., Lehmann, S. C., Meyer, M. T., Dietze, J. E., & Griffith, C. B. (2016). Cyanotoxins in inland lakes of the United States: Occurrence and potential recreational health risks in the EPA National Lakes Assessment 2007. *Harmful Algae*, *56*, 77–90. https://doi.org/10.1016/j.hal.2016.04.001

Lopez Barreto, B. (2023). Data and materials for Lopez Barreto et al. (2023) [Dataset]. Mendeley Data, V4. https://doi.org/10.17632/vthwsyyhb3.3

Lunetta, R. S., Schaeffer, B. A., Stumpf, R. P., Keith, D., Jacobs, S. A., & Murphy, M. S. (2015). Evaluation of cyanobacteria cell count detection derived from MERIS imagery across the eastern USA. *Remote Sensing of Environment*, *157*, 24–34. https://doi.org/10.1016/j.rse.2014.06.008

Matthews, M. (2014). Eutrophication and cyanobacterial blooms in South African inland waters: 10 years of MERIS observations. *Remote Sensing of Environment*, *155*, 161–177. https://doi.org/10.1016/j.rse.2014.08.010

Matthews, M., & Bernard, S. (2015). Eutrophication and cyanobacteria in South Africa's standing water bodies: A view from space. *South African Journal of Science*, *111*(5/6), 1–8. https://doi.org/10.17159/sajs.2015/20140193

Mishra, S., & Mishra, D. R. (2012). Normalized difference chlorophyll index: A novel model for remote estimation of chlorophyll-a concentration in turbid productive waters. *Remote Sensing of Environment*, *117*, 394–406. https://doi.org/10.1016/j.rse.2011.10.016

Mishra, S., Stumpf, R. P., Schaeffer, B., Werdell, P. J., Loftin, K. A., & Meredith, A. (2021). Evaluation of a satellite-based cyanobacteria bloom detection algorithm using field-measured microcystin data. *Science of the Total Environment*, *774*, 145462. https://doi.org/10.1016/j.scitotenv.2021.145462

Mobley, C., Werdell, J., Franz, B., Ahmad, Z., & Bailey, S. (2016). Atmospheric correction for satellite ocean color radiometry. https://doi.org/10.13140/RG.2.2.23016.78081

Moore, G. K. (1980). Satellite remote sensing of water turbidity/Sonde de télémesure par satellite de la turbidité de l'eau. *Hydrological Sciences Bulletin*, *25*(4), 407–421. https://doi.org/10.1080/02626668009491950

Moses, W. J., Gitelson, A. A., Berdnikov, S., Saprygin, V., & Povazhnyi, V. (2012). Operational MERIS-based NIR-red algorithms for estimating chlorophyll-a concentrations in coastal waters—The Azov Sea case study. *Remote Sensing of Environment*, *121*, 118–124. https://doi.org/10.1016/j.rse.2012.01.024

NASA Ocean Biology Processing Group. (2023). Cyanobacteria assessment network (CyAN) level-3 ocean color data, version 4. Retrieved from https://oceandata.sci.gsfc.nasa.gov/api/cyan_file_search

Nechad, B., Ruddick, K. G., & Neukermans, G. (2009). Calibration and validation of a generic multisensor algorithm for mapping of turbidity in coastal waters. *Proceedings of SPIE*, *7473*, 161–171. https://doi.org/10.1117/12.830700

New Jersey Department of Environmental Protection (NJDEP). (2020). Cyanobacterial harmful algal bloom (HAB) freshwater recreational response strategy. Retrieved from https://www.state.nj.us/dep/hab/download/NJHABResponseStrategy.pdf

OEHHA. (2012). *Toxicological summary and suggested action levels to reduce potential adverse health effects of six cyanotoxins*. Office of Environmental Health Hazard Assessment, California Environmental Protection Agency. Retrieved from http://www.swrcb.ca.gov/water_issues/programs/peer_review/docs/calif_cyanotoxins/cyanotoxins053112.pdf

Oregon Health Authority (OHA). (2023). Public health division. Recreational use public health advisory guidelines for cyanobacterial blooms in freshwater bodies. Retrieved from https://www.oregon.gov/oha/ph/HealthyEnvironments/Recreation/HarmfulAlgaeBlooms/Pages/BlueGreenAlgaeAdvisories.aspx

O'Reilly, J. E., & Werdell, P. J. (2019). Chlorophyll algorithms for ocean color sensors—OC4, OC5 & OC6. *Remote Sensing of Environment*, *229*, 32–47. https://doi.org/10.1016/j.rse.2019.04.021

Paerl, H. W., Hall, N. S., & Calandrino, E. S. (2011). Controlling harmful cyanobacterial blooms in a world experiencing anthropogenic and climatic-induced change. *Science of the Total Environment*, *409*(10), 1739–1745. https://doi.org/10.1016/j.scitotenv.2011.02.001

Pahlevan, N., Smith, B., Schalles, J., Binding, C., Cao, Z., Ma, R., et al. (2020). Seamless retrievals of chlorophyll-a from Sentinel-2 (MSI) and Sentinel-3 (OLCI) in inland and coastal waters: A machine-learning approach. *Remote Sensing of Environment*, *240*, 111604. https://doi.org/10.1016/j.rse.2019.111604

Papenfus, M., Schaeffer, B., Pollard, A. I., & Loftin, K. (2020). Exploring the potential value of satellite remote sensing to monitor chlorophyll-a for US lakes and reservoirs. *Environmental Monitoring and Assessment*, *192*(12), 808. https://doi.org/10.1007/s10661-020-08631-5

Randolph, K., Wilson, J., Tedesco, L., Li, L., Pascual, D. L., & Soyeux, E. (2008). Hyperspectral remote sensing of cyanobacteria in turbid productive water using optically active pigments, chlorophyll a and phycocyanin. *Remote Sensing of Environment*, *112*(11), 4009–4019. https://doi.org/10.1016/j.rse.2008.06.002

Rodríguez-Benito, C. V., Navarro, G., & Caballero, I. (2020). Using Copernicus Sentinel-2 and Sentinel-3 data to monitor harmful algal blooms in Southern Chile during the COVID-19 lockdown. *Marine Pollution Bulletin*, *161*, 111722. https://doi.org/10.1016/j.marpolbul.2020.111722

Ruiz-Verdú, A., Simis, S. G. H., de Hoyos, C., Gons, H. J., & Peña-Martínez, R. (2008). An evaluation of algorithms for the remote sensing of cyanobacterial biomass. *Remote Sensing of Environment*, *112*(11), 3996–4008. https://doi.org/10.1016/j.rse.2007.11.019

Santa Clara Valley Water. (2023). Imported water: Vital to Santa Clara county. Retrieved from https://www.valleywater.org/your-water/where-your-water-comes/imported-water

Schaeffer, B. A., Bailey, S. W., Conmy, R. N., Galvin, M., Ignatius, A. R., Johnston, J. M., et al. (2018). Mobile device application for monitoring cyanobacteria harmful algal blooms using Sentinel-3 satellite ocean and Land Colour Instruments. *Environmental Modelling & Software*, *109*, 93–103. https://doi.org/10.1016/j.envsoft.2018.08.015

Schaeffer, B. A., Urquhart, E., Coffer, M., Salls, W., Stumpf, R. P., Loftin, K. A., & Jeremy Werdell, P. (2022). Satellites quantify the spatial extent of cyanobacterial blooms across the United States at multiple scales. *Ecological Indicators*, *140*, 108990. https://doi.org/10.1016/j.ecolind.2022.108990

Seegers, B. N., Werdell, P. J., Vandermeulen, R. A., Salls, W., Stumpf, R. P., Schaeffer, B. A., et al. (2021). Satellites for long-term monitoring of inland U.S. lakes: The MERIS time series and application for chlorophyll-a. *Remote Sensing of Environment*, *266*, 112685. https://doi.org/10.1016/J.RSE.2021.112685

Sendersky, E., Simkovsky, R., Golden, S., & Schwarz, R. (2017). Quantification of chlorophyll as a proxy for biofilm formation in the cyanobacterium synechococcus elongatus. *Bio-Protocol*, *7*(14). https://doi.org/10.21769/BioProtoc.2406

Sharp, S. L., Forrest, A. L., Bouma-Gregson, K., Jin, Y., Cortés, A., & Schladow, S. G. (2021). Quantifying scales of spatial variability of cyanobacteria in a large, eutrophic lake using multiplatform remote sensing tools. *Frontiers in Environmental Science*, *9*. https://doi.org/10.3389/fenvs.2021.612934

Sklenar, K., Westrick, J., & Szlag, D. (2016). Managing cyanotoxins in drinking water: A technical guidance manual for drinking water professionals. Retrieved from https://www.awwa.org/Portals/0/AWWA/ETS/Resources/TechnicalReports/201609_Managing_Cyanotoxins_In_Drinking_Water.pdf?ver=2021-05-21-120350-733

Smayda, T. J. (1997). Harmful algal blooms: Their ecophysiology and general relevance to phytoplankton blooms in the sea (Vol. *42*).

Stirbet, A., Lazar, D., Kromdijk, J., & Govindjee, G. (2018). Chlorophyll a fluorescence induction: Can just a one-second measurement be used to quantify abiotic stress responses? *Photosynthetica*, *56*, 86–104. https://doi.org/10.1007/s11099-018-0770-3

Stroming, S., Robertson, M., Mabee, B., Kuwayama, Y., & Schaeffer, B. (2020). Quantifying the human health benefits of using satellite information to detect cyanobacterial harmful algal blooms and manage recreational advisories in U.S. Lakes. *GeoHealth*, *4*(9), e2020GH000254. https://doi.org/10.1029/2020GH000254

Stumpf, R. P., Davis, T. W., Wynne, T. T., Graham, J. L., Loftin, K. A., Johengen, T. H., et al. (2016). Challenges for mapping cyanotoxin patterns from remote sensing of cyanobacteria. *Harmful Algae*, *54*, 160–173. https://doi.org/10.1016/j.hal.2016.01.005

Stumpf, R. P., & Tomlinson, M. C. (2007). In R. L. Miller, C. E. Del Castillo, & B. A. Mckee (Eds.), *Remote sensing of harmful algal blooms BT—Remote sensing of coastal aquatic environments: Technologies, techniques and applications*. https://doi.org/10.1007/978-1-4020-3100-7_12

Tebbs, E. J., Remedios, J. J., & Harper, D. M. (2013). Remote sensing of chlorophyll-a as a measure of cyanobacterial biomass in Lake Bogoria, a hypertrophic, saline–alkaline, flamingo lake, using Landsat ETM+. *Remote Sensing of Environment*, *135*, 92–106. https://doi.org/10.1016/j.rse.2013.03.024

Theenathayalan, V., Sathyendranath, S., Kulk, G., Menon, N., George, G., Abdulaziz, A., et al. (2022). Regional satellite algorithms to estimate chlorophyll-a and total suspended matter concentrations in Vembanad Lake. *Remote Sensing*, *14*(24), 6404. https://doi.org/10.3390/rs14246404

Tomlinson, M. C., Stumpf, R. P., Wynne, T. T., Dupuy, D., Burks, R., Hendrickson, J., & Fulton, R. S., III. (2016). Relating chlorophyll from cyanobacteria-dominated inland waters to a MERIS bloom index. *Remote Sensing Letters*, *7*(2), 141–149. https://doi.org/10.1080/2150704X.2015.1117155

Tóth, V. Z., Ladányi, M., & Jung, A. (2021). Adaptation and validation of a Sentinel-based chlorophyll-a retrieval software for the central European freshwater lake, Balaton. *PFG—Journal of Photogrammetry, Remote Sensing and Geoinformation Science*, *89*(4), 335–344. https://doi.org/10.1007/s41064-021-00160-1

United States Bureau of Reclamation. (2023). California-Great Basin, Central Valley Project. Retrieved from https://www.usbr.gov/mp/cvp/

United States Environmental Protection Agency. (2023). Detection methods for cyanotoxins. Retrieved from https://www.epa.gov/ground-water-and-drinking-water/detection-methods-cyanotoxins

Urquhart, E. A., Schaeffer, B. A., Stumpf, R. P., Loftin, K. A., & Werdell, P. J. (2017). A method for examining temporal changes in cyanobacterial harmful algal bloom spatial extent using satellite remote sensing. *Harmful Algae*, *67*, 144–152. https://doi.org/10.1016/J.HAL.2017.06.001

Vanhellemont, Q. (2019). Adaptation of the dark spectrum fitting atmospheric correction for aquatic applications of the Landsat and Sentinel-2 archives. *Remote Sensing of Environment*, *225*, 175–192. https://doi.org/10.1016/j.rse.2019.03.010

Vanhellemont, Q., & Ruddick, K. (2018). Atmospheric correction of metre-scale optical satellite data for inland and coastal water applications. *Remote Sensing of Environment*, *216*, 586–597. https://doi.org/10.1016/j.rse.2018.07.015

Werther, M., Odermatt, D., Simis, S. G. H., Gurlin, D., Lehmann, M. K., Kutser, T., et al. (2022). A Bayesian approach for remote sensing of chlorophyll-a and associated retrieval uncertainty in oligotrophic and mesotrophic lakes. *Remote Sensing of Environment*, *283*, 113295. https://doi.org/10.1016/j.rse.2022.113295

Wolf, D., Georgic, W., & Klaiber, H. A. (2017). Reeling in the damages: Harmful algal blooms' impact on Lake Erie's recreational fishing industry. *Journal of Environmental Management*, *199*, 148–157. https://doi.org/10.1016/j.jenvman.2017.05.031

Wynne, T. T., Stumpf, R. P., Tomlinson, M. C., & Dyble, J. (2010). Characterizing a cyanobacterial bloom in Western Lake Erie using satellite imagery and meteorological data. *Limnology & Oceanography*, *55*(5), 2025–2036. https://doi.org/10.4319/lo.2010.55.5.2025

Wynne, T. T., Stumpf, R. P., Tomlinson, M. C., Warner, R. A., Tester, P. A., Dyble, J., & Fahnenstiel, G. L. (2008). Relating spectral shape to cyanobacterial blooms in the Laurentian Great Lakes. *International Journal of Remote Sensing*, *29*(12), 3665–3672. https://doi.org/10.1080/01431160802007640

Wyoming Department of Environmental Quality (WDEQ). (2022). Water quality division, harmful cyanobacterial bloom action plan for publicly accessible lakes and reservoirs of wyoming. Retrieved from https://deq.wyoming.gov/2022/06/notice-to-avoid-and-report-possible-harmful-cyanobacterial-blooms-in-wyoming-waters-3/